

## Supplemental Material

### Gene Expression Differences after Rituximab Treatment.

Skin biopsies were first analyzed from dSSc patients before and after treatment with rituximab. Consistent with the clinical findings (Lafyatis *et al.*, 2009), we did not find a significant gene expression response in skin to rituximab treatment. Instead, gene expression was nearly identical between serial biopsies of patients before and after treatment.

RNA was isolated from skin biopsies of 13 patients enrolled in the rituximab study and hybridized to whole-genome DNA microarrays. Lesional forearm samples were analyzed from 10 patients before treatment (base) and six months after rituximab treatment. Non-lesional back skin biopsies were analyzed for 4 of the 10 patients at base and six months. Patient 7 provided forearm and back biopsies eight months before rituximab therapy (pre-base). Patient 17 provided an additional forearm biopsy at twenty months after therapy. Patient 10 provided a forearm biopsy at thirty months after therapy. A total of 49 arrays were analyzed for the rituximab dataset, including 12 technical replicates.

Significance Analysis of Microarrays (SAM) was used to identify differences in gene expression before and after rituximab treatment (Tusher *et al.*, 2001). Two different comparisons were performed. One analysis compared the gene expression of base and six-month time points in forearm biopsies alone. Only 17 probes were significantly differentially expressed at a false discovery rate (FDR) 4.6% (**Supplemental Data File S1**). Inclusion of the non-lesional back samples in the above analysis resulted in 16 probes significantly differentially expressed at an FDR 5.87%.

As a second approach, we selected probes with the most consistent expression at a single time point (such as base) for each patient but the most diverse expression between time points. This analysis identified genes/probes that most varied after treatment. We refer to this as an ‘Intrinsic by Time Point’ analysis, as all samples at a single time point for a patient were

considered an independent group. This is distinct from an ‘Intrinsic by Patient Analysis’ (Milano *et al.*, 2008; Perou *et al.*, 2000; Sorlie *et al.*, 2001), where all samples from a given patient are considered an independent group, regardless of the time point of biopsy collection. 1255 probes were selected with intrinsic scores  $< 0.35$  (FDR 2.5%), and were hierarchically clustered by gene and by array. Despite selecting specifically for probes with expression most variable between time points, arrays for 6 months and base for each patient grouped together (**Supplemental Figure S2A**). In addition, skin biopsies taken at 14, 20 and 24 months from patients 7, 10, and 17, respectively, also grouped with the base and 6-month samples. This demonstrates consistent gene-expression for up to 2 years after the initial biopsy in patients treated with rituximab.

Finally, we asked if we could identify gene expression changes that correlated with the decrease in the numbers of B cells present in the skin of patients treated with rituximab, as determined by immunohistochemistry (IHC). Probes were selected with the strongest correlation between decreased gene expression and CD20+ B cell depletion in the skin after rituximab treatment. A total of 119 probes were selected with correlations  $> 0.50$ . The 119 probes generally show low expression levels (**Supplemental Figure 2B; Supplemental Data File S2**). There is a weak enrichment for genes typically associated with B-cells such as LCP1 which is a membrane expressed protein restricted to hematopoietic stem cell lineages (Samstag and Klemke, 2007) and TNFRSF8 (CD30) expressed only on mitogen-activated B cells and T cells (Falini *et al.*, 1995).

These results show few gene expression differences were found in SSc skin after rituximab treatment. This is consistent with the observation that the mean change in MRSS for rituximab treated patients was not significantly different between baseline (20.6) and 6-months (20.2). The most important observation from this analysis is the similarity of gene expression from 6 months to 2 years, in dSSc patients with early and active disease.

### Concordance in biological pathways.

The module map was generated using GO Biological Process and Molecular Function gene sets, as well as gene sets representing cell cycle-regulated genes (Whitfield *et al.*, 2002) (**Supplemental Figure S3**). Modules with increased expression are shown in red; those with decreased expression are shown in green ( $p \leq 0.05$ , FDR correction 0.1). Modules were clustered in the gene dimension by similarity of expression, and arrays were ordered as in the by patient analysis presented in **Figure 2**.

Patients in the inflammatory group show coordinate increased expression of genes involved in inflammatory response, angiogenesis, antigen processing, and chemokine receptor activity. The diffuse 2 proliferation group shows increased expression of cell cycle-related gene sets including those for S, G2, and G2/M phases of the cell cycle. The diffuse 1 proliferation group shows a weak increase in proliferation related signatures. The normal-like group and diffuse 1 proliferation group show increased expression of genes associated with lipid metabolism and fatty acid metabolism. The module map with all GO biological processes is available in **Supplemental Figure S4**.

The skin is comprised of many different cell types, and the inflammatory signature in part results from infiltrating mononuclear cells (Milano *et al.*, 2008), thus additional gene sets for specific cell types were collected from the published literature and used with Genomica analysis. We collected genes sets for B cells, T cells, and granulocytes (Palmer *et al.*, 2006), as well as gene sets for isolated fibroblasts, keratinocytes, macrophages, monocytes, and immature and mature dendritic cells (Haider *et al.*, 2008). Haider *et al.* also identified genes upregulated after keratinocytes were treated with interferon-gamma (INF- $\gamma$ ) and with tumor necrosis factor (TNF), and characterized gene expression changes in anti-CD3/CD28 treated T cells and PBMCs. In addition they created gene sets for upregulated genes in combined groups of cells, including myeloid cells (DC, macrophages, monocytes), skin resident cells (fibroblasts and keratinocytes), and leukocytes (monocytes, macrophages, DCs, and T cells).

Genomic analysis using these cell type-specific gene sets ( $p \leq 0.05$ , FDR 0.1) shows highest coordinate increased expression associated with fibroblasts, keratinocytes, activated keratinocytes and fibroblasts, activated PBMCs, and other infiltrating circulating cells in the inflammatory group (**Supplemental Figure S3B**). Also apparent is the coordinate increased expression of genes associated with activated monocytes, T cells and genes with peak expression at G1/S, G2, G2/M, and S phase. There was coordinate upregulation for myeloid cells and mature and immature dendritic cells (DCs) for SSc patients compared to healthy controls.

## **Supplemental Materials and Methods.**

### **Patient biopsies**

A total of 60 skin biopsies were collected from 22 patients with dSSc and 9 healthy controls. Each biopsy was placed in RNAlater (Ambion) and stored at -20 until processed. Lesional forearm samples were analyzed from ten patients enrolled in the rituximab study before treatment (base) and six months after rituximab treatment. One individual (Patient 7) provided forearm and back biopsies eight months before rituximab therapy (pre-base). Another (Patient 17) provided an additional forearm biopsy at 20 months after therapy. A third (Patient 10) provided a forearm biopsy at 30 months after therapy. Two patients who were not treated with rituximab were biopsied at 10 and 6 months after baseline (Non-RIT1 and Non-RIT2 respectively).

### **RNA and Microarray Processing**

The Agilent low input fluorescent linear amplification kit was used to fluorescently label and amplify 100ng total RNA for hybridization. Subject RNA was labeled with Cy3 dye, and Universal Human Reference RNA (UHR) (Stratagene) was labeled with fluorescent Cy5 dye. After amplification and labeling, the cRNA was purified using the Qiagen RNeasy mini spin columns and procedure. Patient or normal-control RNA was co-hybridized with UHR RNA to 4-



plex 44K Agilent 60-mer whole human genome microarrays, representing 41,000 unique probes.

The hybridization was carried out for 17 hours at 65°C.

Arrays were washed using the two-color microarray-based gene expression analysis protocol for use with the Agilent Stabilization and Drying Solution (6X SSPE, 0.005% N-Lauroylsarcosine for 1 minute at room temperature; 0.06X SSPE, 0.005% N-Lauroylsarcosine for 1 minute at 37°C; Acetonitrile wash for 1 minute at room temperature; Stabilization and Drying Solution for 30 seconds at room temperature). A total of 89 arrays were hybridized, which included 29 technical replicates.

A dual laser GenePix 4000B scanner (Axon Instruments) was used to scan the arrays. Gene Pix Pro 5.0 software was used to inspect arrays, and spots showing irregularities were manually flagged and excluded. The data was Log<sub>2</sub> LOWESS normalized for the Cy5/Cy3 ratio. The data was filtered to select array spots with an intensity 2 fold or greater than the local background in either the Cy3 or Cy5 channel. Any probes missing more than 20% of the data across all arrays were also omitted from further analysis.

### **Intrinsic gene analysis**

Intrinsic gene analysis is essentially a ‘within-between’ comparison of the gene expression of individual probes. The method is used to identify probes with gene expression most similar within each group of arrays (arrays grouped either ‘by patient time point’ or ‘by patient’), but gene expression most variable between groups of arrays. Filtering probes in this way reduces the variability between arrays, in order to better compare the gene expression between groups and/or patients. For the gene expression of each probe, the algorithm calculated the ratio of the variability within each group of arrays, divided by the variability between each group of arrays. The weighted average of the variance of each group of arrays formed the value of the numerator (A). The weighted average of the gene expression for arrays in each group was calculated and the variance of the average gene expression across all groups of arrays formed the

denominator (B). As a result, the smaller the expression variance within each individual group of arrays, and the larger the expression variance between groups, the smaller the “intrinsic score” calculated for each probe.

To determine an FDR value, the gene expression data was permuted 20 times, and the intrinsic gene algorithm was used with each of the permuted gene expression datasets. The average number of probes that were less than a given intrinsic score cutoff in the permuted data was divided by the number of probes that obtained the intrinsic score cutoff in the non-permuted data. This value was multiplied by 100 to provide a percentage FDR rate.

### **DAVID Analysis**

The Database for Annotation, Visualization, and Integrated Discovery tool (DAVID) (Huang *et al.*, 2007) was used to analyze the enrichment of GO biological processes associated with the list of genes in each of the intrinsic ‘by patient’ inflammatory, proliferation, and fatty-acid gene expression subsets. The GO-term pathway results with a Benjamini-hochberg corrected p-value  $\leq 0.1$  are listed in **Supplementary Data File S3**.

### **Hierarchical clustering**

Using cluster 3.0 software, the gene expression data was average linkage hierarchically clustered in the array and gene dimension (<http://bonsai.ims.u-tokyo.ac.jp/~mdehoon/software/cluster/software.htm>). The gene expression data was viewed using Java Tree View (<http://jtreeview.sourceforge.net/>).

### **Module maps**

Module maps were created utilizing Genomica software. The gene sets used within Genomica included the GO biological pathway, process, and function gene sets, as well as gene sets comprised of genes expressed coordinately during various phases of the cell cycle from a study

by Whitfield et al. (Whitfield *et al.*, 2002). Additional gene sets included those for B-cells, T-cells, and granulocytes from Palmer et al. (Palmer, Diehn et al. 2006) as well as those by Haider et al. (Haider, Lowes et al. 2008) who defined a number of unique sets of genes for various cell types, used here to create gene sets for Genomica analysis. Haider et al. collected a series of microarray experiments that detected up-regulation of gene expression for isolated fibroblasts, keratinocytes, macrophages, monocytes, and immature and mature dendritic cells. They created also gene lists from genes upregulated after keratinocytes were treated with interferon-gamma (INF- $\gamma$ ) and with tumor necrosis factor (TNF). They also characterized gene expression changes in CD3/CD28 activated T cells and PBMCs. In addition they formed lists of genes showing up regulation in expression associated with overlapping groups of cells, including myeloid cells (DC, macrophages, monocytes) as well as skin resident cells (fibroblasts and keratinocytes), and leukocytes (monocytes, macrophages, DCs, and T cells).

### **Immunohistochemistry**

Formalin fixed, paraffin embedded sections were rehydrated and either treated for antigen retrieval (COMP, 8 minutes in pressure cooker in 1X CitraPlus, Biogenex) or stained without antigen retrieval (IFITM3). Sections were then treated for 45 minutes with 0.3% peroxide, blocked in 3% BSA for 30 minutes and incubated with primary antibody to IFITM3 (rabbit anti-human IFITM3, Epitomics, clone EPR5242) 1:250 dilution, or COMP (rabbit anti-human COMP, Epitomics polyclonal, cat# T1833) 1:100 dilution at 4 °C overnight, these reagents all diluted into 1X Tris buffered saline (pH 7.4, Fisher) supplemented with 0.1% Tween20. The following day secondary reagent was applied (ImmPRESS Universal Reagent, Anti-mouse/rabbit Ig, Peroxidase, Vector Laboratories), developed (ImmPACT DAB, Vector) and counterstained with Hematoxylin. Staining was scored by a blinded observer on a 0-100 point visual analog scale as described previously (Farina *et al.*)

**Supplemental Table 1. Skin Biopsies Analyzed**

Subject	Base	6 Months	Additional Biopsy	Notes
RIT 2		X		Back sample only
RIT 3	X	X		
RIT 5	X	X		
RIT 6	X	X		
RIT 7	X	X	8 months before base	No back sample for base biopsy
RIT 8	X	X		No forearm sample for base biopsy
RIT 10		X	30 months after base	Forearm only
RIT 11	X	X		
RIT 12	X	X		Forearm only
RIT 13	X	X		Forearm only
RIT 14	X	X		Forearm only
RIT 15	X	X		Forearm only
RIT 17	X	X	20 months after base	Forearm only
dSSc non RIT 1	X		10 months later	Forearm only
dSSc non RIT 2	X	X		Forearm only
dSSc non RIT 3	X			
dSSc non RIT 4	X			
dSSc non RIT 5	X			Forearm only
dSSc non RIT 6	X			Forearm only
dSSc non RIT 7	X			Forearm only
dSSc non RIT 8	X			Forearm only
dSSc non RIT 9	X			Forearm only
Normal 1	X			Forearm only
Normal 2	X			Forearm only
Normal 3	X			Forearm only
Normal 4	X			Forearm only
Normal 5	X			Forearm only
Normal 6	X			Forearm only
Normal 7	X			Forearm only
Normal 8	X			Forearm only
Normal 9	X			Forearm only

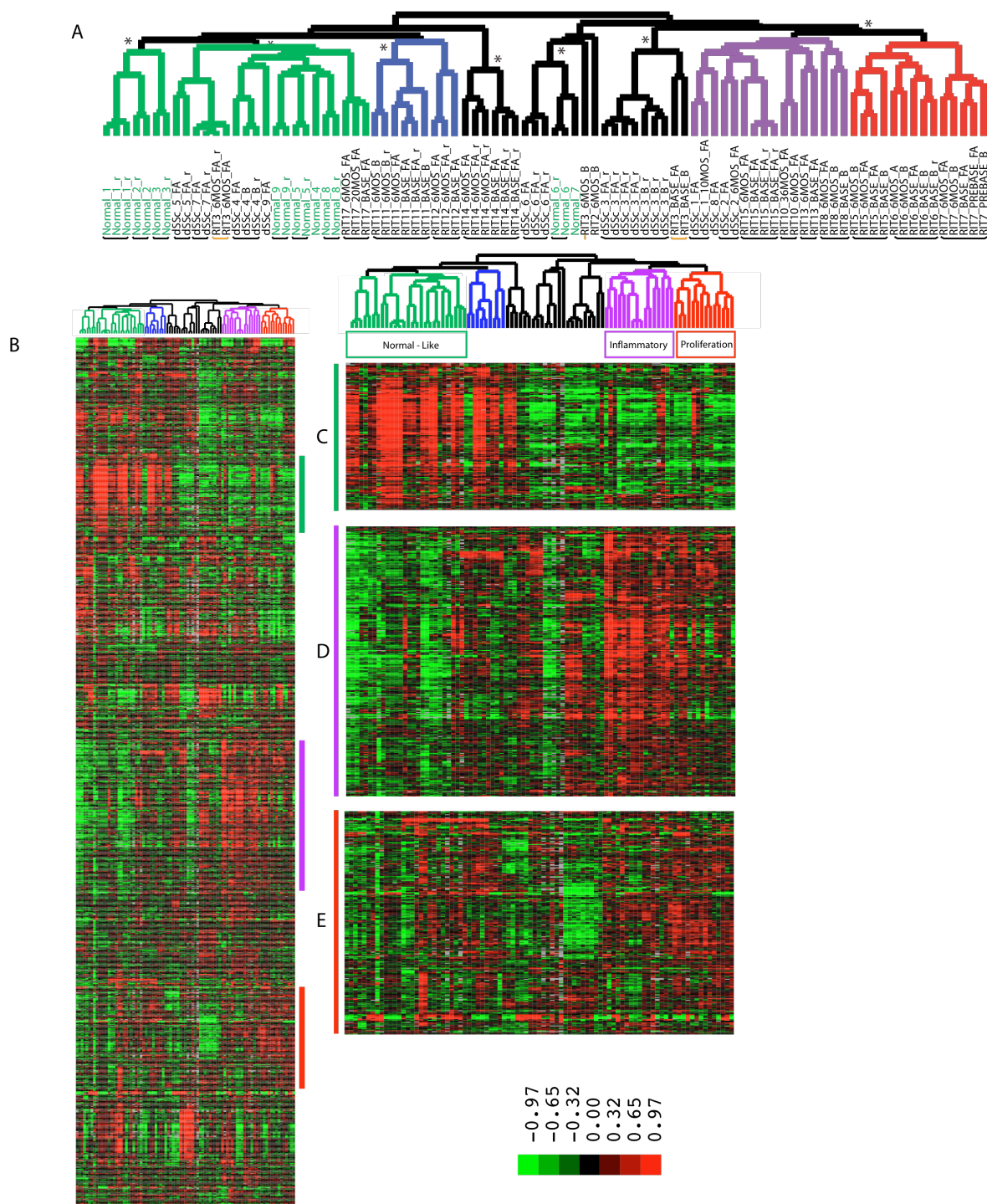
Skin biopsy samples, indicating if samples were collected at base, 6 months later, if only forearm (lesional) skin was collected, and if any additional samples were collected.

Supplemental Table S2: Subject Clinical Characteristics

Subject	Age <sup>1</sup> / Sex	Biopsy Interval	Disease Duration (months)	MRSS	FVC	DLCO	Autoantibodies Scl-70 /RNApoIII/CENPB	Intrinsic Subset Assignment <sup>2</sup>	Medications
RIT 2	54/F	base	18	27.5	62	61	+ / - / -	Unclassified	
		6 months	24	28	85	72			PREDNISON 5 MG, RITUXIMAB
RIT 3	42/F	base	18	13	72	55	+ / - / -	Unclassified	
		6 months	24	13	76	56			RITUXIMAB
RIT 5	32/F	base	18	19	108	80	- / - / -	Diffuse 2	PLAQUENIL
		6 months	24	23	108	74			PLAQUENIL RITUXIMAB
RIT 6	49/F	base	15	27.5	117	98	- / - / -	Diffuse 2	PREDNISON 5 MG
		6 months	21	25	112	87			RITUXIMAB
RIT 7	46/F	pre base	7	19			- / - / -	Diffuse 2	
		base	15	19	86	85	- / + / -	Diffuse 2	METHOTREXATE, PREDNISON 5 MG
		6 months	21	15	100	86			METHOTREXATE, PREDNISON, RITUXIMAB
RIT 8	53/F	base	18	31	94	81	- / + / -	Inflammatory	
		6 months	24	45.5	93	76			RITUXIMAB
RIT 10	38/F	base	12	10	83	107	- / - / -	Inflammatory	PLAQUENIL, PREDNISON 5 MG
		6 months	18	7	101	85			PLAQUENIL PREDNISON RITUXIMAB
		36 months	42	20	92	74			Bosentan, Avapro
RIT 11	36/M	base	15	29	64	78	- / - / -	Diffuse 1	PREDNISON 5 MG,
		6 months	21	29	53	69			PREDNISON, RITUXIMAB
RIT 12	33/F	base	18	15	105	67	+ / - / -	Diffuse 1	
		6 months	24	15	105	95			RITUXIMAB
RIT 13	56/F	base	11	13	119	81	- / + / -	Inflammatory	
		6 months	17	17	100	84			RITUXIMAB
RIT 14	43/F	base	9	9	76	66	- / - / +	Unclassified	
		6 months	15	5	71	52			RITUXIMAB
RIT 15	44/F	base	7	20	102	94	- / - / -	Inflammatory	
		6 months	13	24	120	94			RITUXIMAB
RIT 17	57/M	base	11	30	78	78	- / - / -	Diffuse 1	
		6 months	18	25	92	87			RITUXIMAB
		25 months	31	17	85	82			
dSSc_3	65/F	base	12	30	66	55	- / ND / ND	Inflammatory	METHREXATE
dSSc_4	54/M	base	26	40	47	30	ND	Diffuse 1	CYCLOPHOSPHAMIDE
dSSc_5	30/F	base	60	24			ND	Normal-like	PREDNISON 5 MG
dSSc_6	53/F	base	48	14	104	102	ND	Inflammatory	MYCOPHENOLATE
dSSc_1	42/M	base	18	40	108	92	- / ND / ND	Inflammatory	NO
		10 months	28	48	103	82			CYCLOPHOSPHAMIDE
dSSc_2	49/F	base	13	37	92	65	ND	Inflammatory	PREDNISON 5 mg,
		6 months	19	35	95	65			
dSSc_7	54/F	base	9	14	79	65	ND	Normal-like	MYCOPHENOLATE
dSSc_8	44/F	base		36	113	74	- / ND / ND	Inflammatory	PREDNISON 5 mg MYCOPHENOLATE
dSSc_9	41/M	base	14	23	60	49	- / ND / ND	Diffuse 1	PREDNISON 5 MG

<sup>1</sup>Age at first biopsy<sup>2</sup>This study

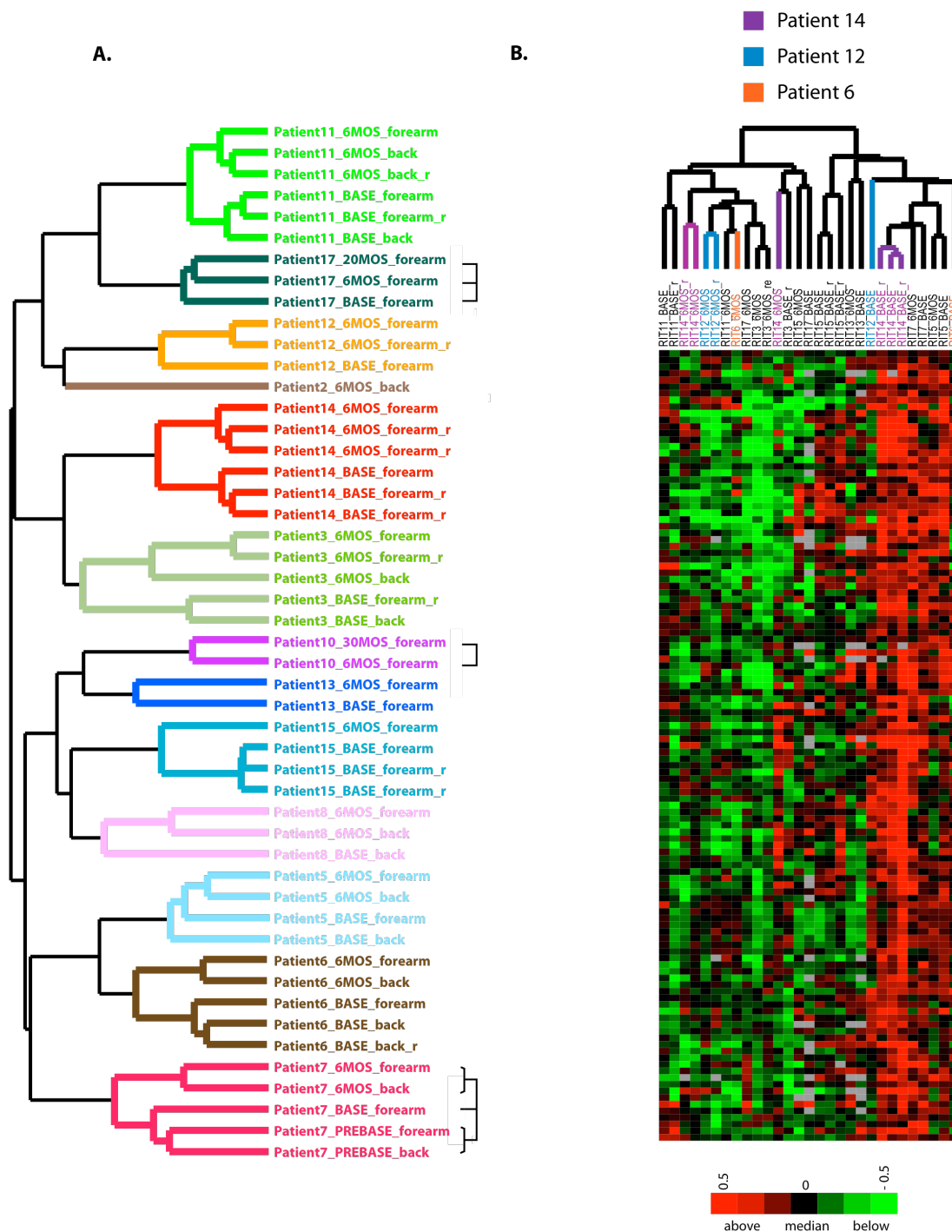
Figure S1

\*  $P < .05$ 

**Supplemental Figure S1. ‘Intrinsic-by-time-point’ analysis shows consistent gene expression between time points. A and B show the results of intrinsic “by patient date” analysis, a resultant 1888 probes with an intrinsic score less than 0.45 (FDR 1.58%) selected**

from 89 arrays and a total of 31 individuals. A. Experimental sample hierarchical clustering dendrogram. Dendrogram branches in green are the '*normal-like*' group, branches in blue (*diffuse 1*) and red (*diffuse 2*) are the '*diffuse-proliferation*' group, and branches in purple are the '*inflammatory*' group. The statistical significance of the clustering was determined by SigClust. Branches that were significant  $p \leq 0.05$  are indicated by a black asterisk (\*) at the lowest significant branch. Patient identifiers below the dendrogram marked in green are from normal healthy control skin biopsies, identifiers in black are from dSSc skin biopsies. Identifiers with "RIT" are samples from the rituximab study, those with "dSSc" are from diffuse SSc patients not in the rituximab study, and identifiers with "normal" indicate a healthy control skin biopsy. Black bars below the identifiers indicate arrays from skin biopsies from the same patient that clustered together. The yellow bars identify arrays for patient RIT 3 that were not in a single cluster. B. Heat map of the 1888 probes hierarchically clustered by gene and by array. C. The Fatty-Acid synthesis related gene expression cluster. D. The group of probes with upregulated expression associated with inflammatory processes and collagen genes. E. The group of probes that shows enrichment for genes involved in cell cycle and proliferating cells.

## Supplemental



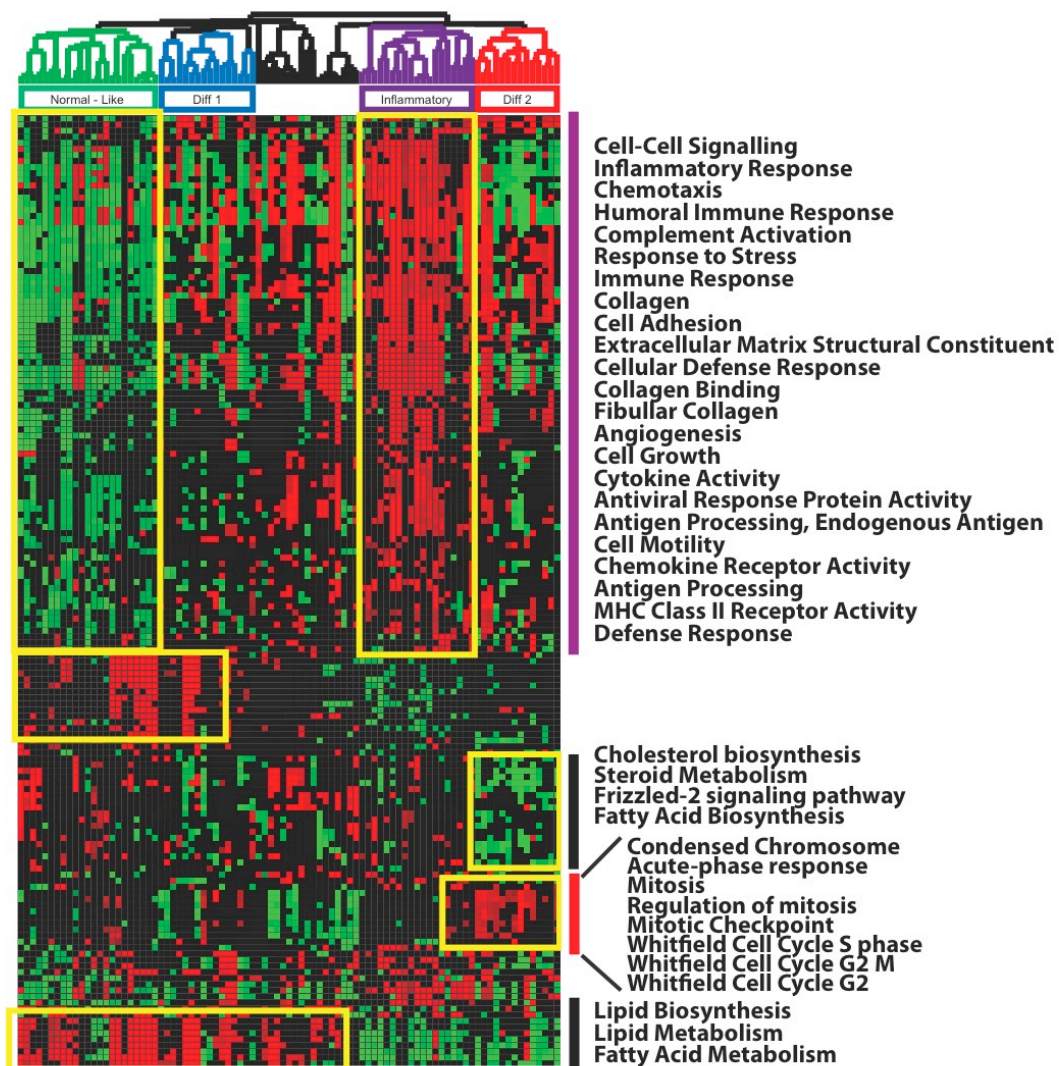
**Supplemental Figure S2. Consistency of gene expression after Rituximab treatment. A.**

The clustering of the group of 1255 probes after intrinsic analysis with samples separated into groups by time point. For each patient, dendrogram branches and sample identifiers are marked

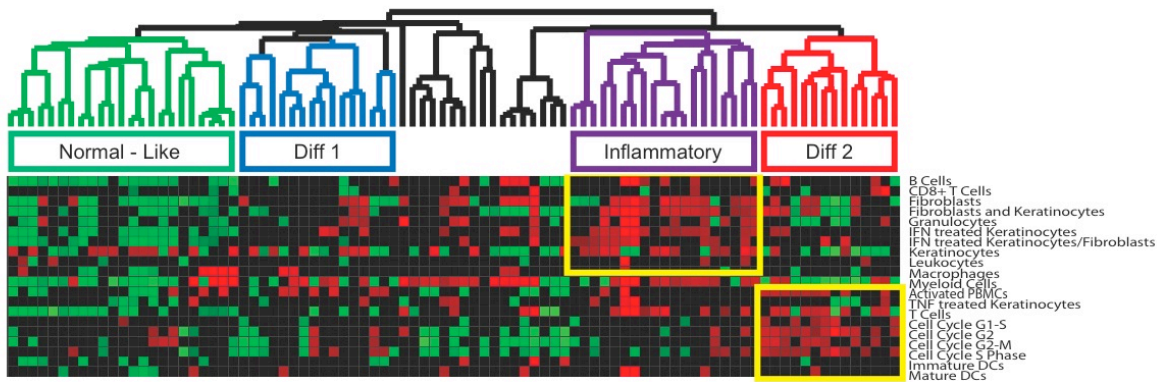


with the same color. Black bars indicate patients with additional skin biopsies beyond base and 6-month samples that clustered with the other arrays. The figure shows consistent clustering between six month and base skin biopsies. Patient 7 (red) had skin biopsies taken eight months before the base sample (prebase), and those biopsies group with the later time point biopsies. Patient10 (purple) had a skin biopsy taken 24 months after the six-month sample, and that array clusters with the 6-month sample. Patient 17 (dark green) had a skin biopsy taken 20 months after the base sample, and again, that array clusters with the earlier time points. This indicates a consistency of gene expression across time points. B. The clustering of the top 119 probes with a positive correlation  $> 0.5$  between gene expression change in forearm skin biopsies and the change in infiltrating CD20+ B-cell number. Patients 14, 12, and 6 (dendrogram branches in purple, blue, and orange respectively) showed weak trends in down regulation of gene expression for the 119 probes between base and 6 months. While patient 14 and patient 6 showed small decreases in skin score, changing from 9 to 5, and 27.5 to 25, respectively, between base and 6 months, patient 12 showed no change in skin score between base and 6 months. In addition, patients 7 and 17 had decreases in skin score between six months and base, and those skin biopsies did not show a change in gene expression between the two time points.

A



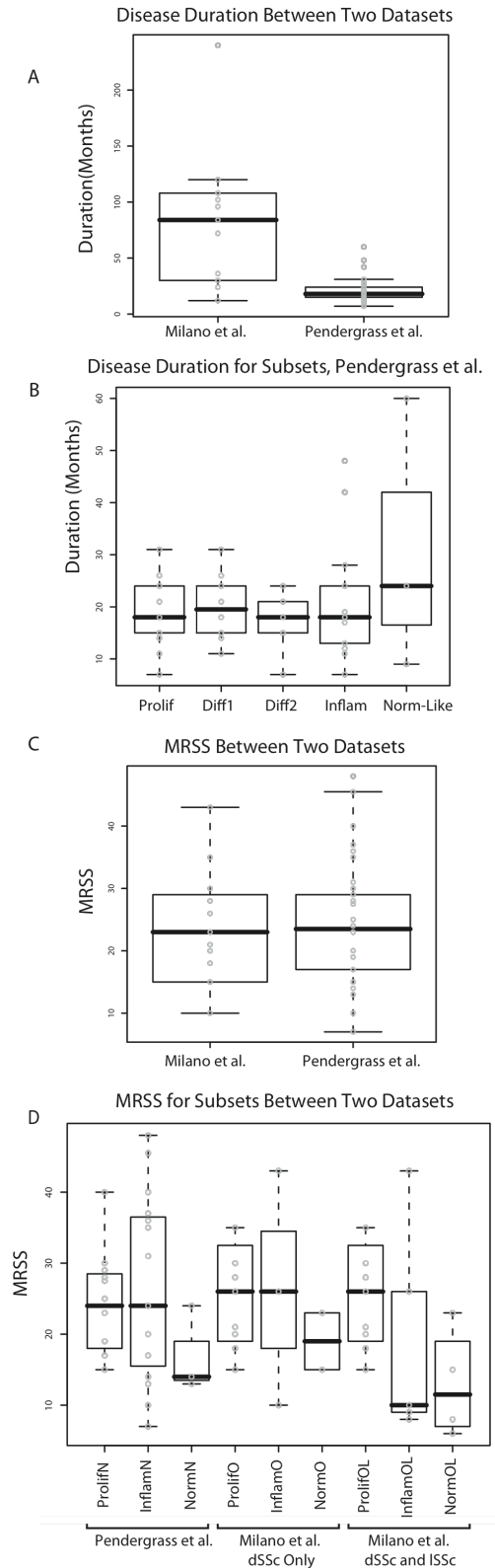
B



**Supplemental Figure S3. Coordinate expression of proliferative, inflammatory, and fatty acid processes.** **A.** The module map representing coordinately regulated genes that correspond to GO biological pathway, process, and function gene sets as well as gene sets expressed coordinately during various phases of the cell cycle. Modules with a significant coordinate increased expression are shown in red; those with decreased expression are shown in green ( $p \leq 0.05$ , FDR correction 0.1). **B.** Module map using gene lists from up-regulated gene expression unique to B cells, T cells, granulocytes, fibroblasts, keratinocytes, macrophages, immature and mature dendritic cells, as well as overlapping groups of cells, including myeloid cells (DC, macrophages, monocytes) as well as skin resident cells (fibroblasts and keratinocytes), and leukocytes (monocytes, macrophages, DCs, and T cells). Also included are pathway related gene lists from microarray analysis of Fibroblasts and Keratinocytes treated with interferon-gamma (INF- $\gamma$ ) or tumor necrosis factor (TNF), as well as gene lists from anti-CD3/CD28 activated PBMCs and T cells.

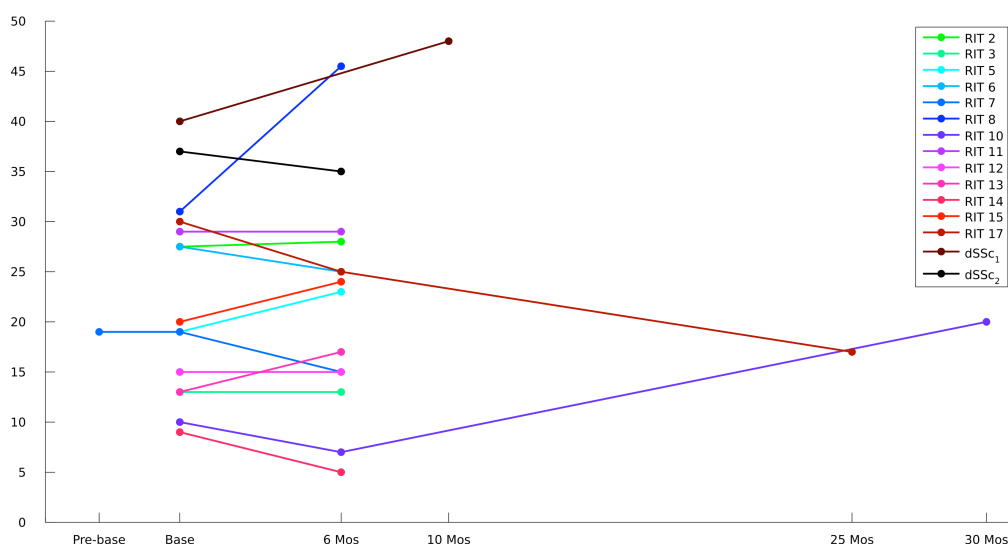


**Supplemental Figure S4. Genomica module map with all GO pathways identified.** The resultant module map representing coordinately regulated genes that correspond to gene sets. Modules with a significant coordinate increased expression are shown in red; those with decreased expression are shown in green ( $p \leq 0.05$ , FDR correction 0.1). This figure is best viewed in PDF format.

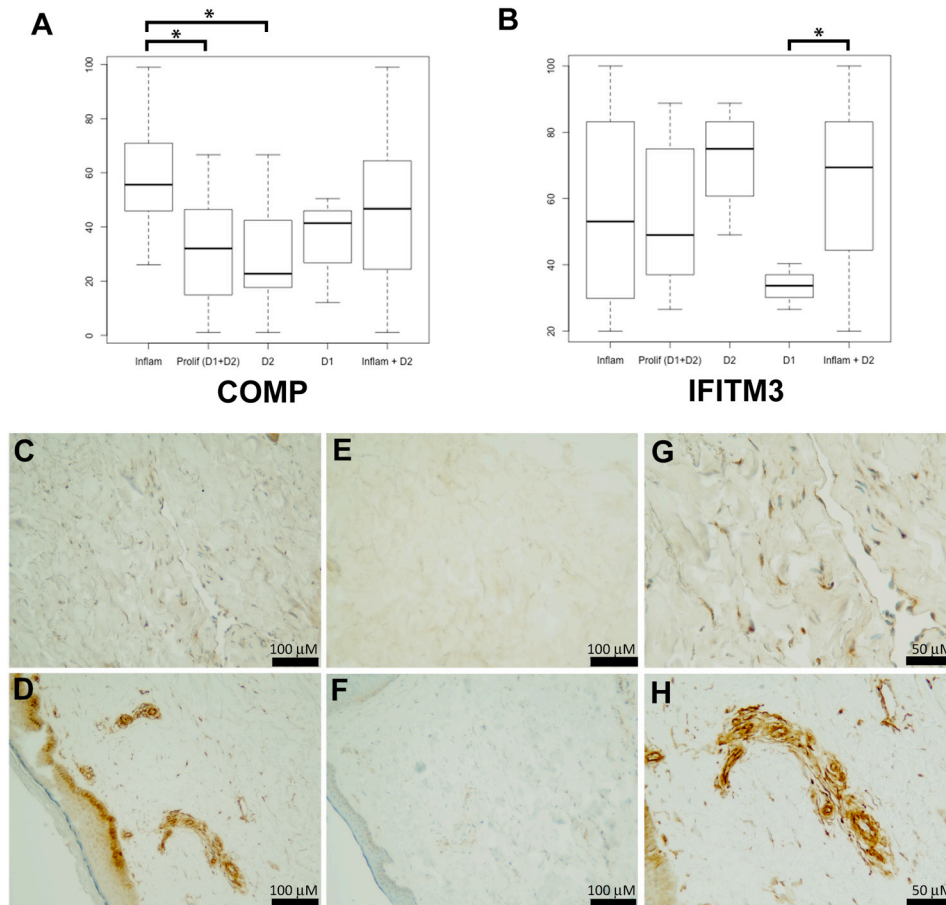


**Supplemental Figure S5. Disease duration different between the two datasets.** **A.** Shows the range of disease duration (in months) between the first and second dataset. **B.** Similarity in median patient disease duration between the ‘intrinsic by patient’ subsets. Although the normal-like group appears to have longer disease duration, the data are skewed by one of three dSSc

patients in this group having a disease duration of 60 months; the opposite trend from what we observed in our previous study (Milano *et al.* 2008). **C.** The range of MRSS skin scores between the first and second dataset. **D.** The range of MRSS for the second dataset split by ‘intrinsic by patient’ subsets (ProlifN, InflanN, NormN), MRSS for the first dataset split by subset when MRSS for limited SSc patients is not included (ProlifO, InflanO, NormO), MRSS for the first dataset when MRSS for limited SSc patients is included (ProlifOL, InflanOL, NormOL).



**Supplemental Figure S6. The MRSS at time of biopsy is plotted for each patient.**



**Supplemental Figure S7. Immunohistochemistry of skin biopsies.** Box plots of the IHC staining results for fifteen skin biopsies spanning the different subsets for COMP (A) which showed highest expression in the inflammatory subset and lowest expression in the proliferation subsets, and eleven biopsies stained for IFITM3 (B) that showed highest expression in the inflammatory and diffuse 2 subset and lowest expression in the diffuse 1 and normal-like groups. Significant differences at  $p < 0.05$  are indicated (\*). A blinded observer scored each biopsy. Representative staining are shown for COMP in SSc (C and G; patient RIT13, 6 month forearm biopsy) and IFITM3 (D and H; patient RIT10, 6 month forearm biopsy). Panels E and F show staining for COMP and IFITM3, respectively in healthy control tissue.



## References

- Falini B, Pileri S, Pizzolo G, Durkop H, Flenghi L, Stirpe F, *et al.* (1995) CD30 (Ki-1) molecule: a new cytokine receptor of the tumor necrosis factor receptor superfamily as a tool for diagnosis and immunotherapy. *Blood* 85:1-14.
- Farina G, Lemaire R, Pancari P, Bayle J, Widom RL, Lafyatis R (2009) Cartilage oligomeric matrix protein expression in systemic sclerosis reveals heterogeneity of dermal fibroblast responses to transforming growth factor beta. *Ann Rheum Dis* 68:435-441.
- Haider AS, Lowes MA, Suarez-Farinas M, Zaba LC, Cardinale I, Blumenberg M, *et al.* (2008) Cellular genomic maps help dissect pathology in human skin disease. *J Invest Dermatol* 128:606-615.
- Huang da W, Sherman BT, Tan Q, Collins JR, Alvord WG, Roayaei J, *et al.* (2007) The DAVID Gene Functional Classification Tool: a novel biological module-centric algorithm to functionally analyze large gene lists. *Genome Biol* 8:R183.
- Lafyatis R, Kissin E, York M, Farina G, Viger K, Fritzler MJ, *et al.* (2009) B cell depletion with rituximab in patients with diffuse cutaneous systemic sclerosis. *Arthritis Rheum* 60:578-583.
- Milano A, Pendergrass SA, Sargent JL, George LK, McCalmont TH, Connolly MK, *et al.* (2008) Molecular subsets in the gene expression signatures of scleroderma skin. *PLoS ONE* 3:e2696.
- Palmer C, Diehn M, Alizadeh AA, Brown PO (2006) Cell-type specific gene expression profiles of leukocytes in human peripheral blood. *BMC Genomics* 7:115.
- Perou CM, Sorlie T, Eisen MB, van de Rijn M, Jeffrey SS, Rees CA, *et al.* (2000) Molecular portraits of human breast tumours. *Nature* 406:747-752.
- Samstag Y, Klemke M (2007) Ectopic expression of L-plastin in human tumor cells: diagnostic and therapeutic implications. *Adv Enzyme Regul* 47:118-126.
- Sorlie T, Perou CM, Tibshirani R, Aas T, Geisler S, Johnsen H, *et al.* (2001) Gene expression patterns of breast carcinomas distinguish tumor subclasses with clinical implications. *Proc Natl Acad Sci U S A* 98:10869-10874.
- Tusher VG, Tibshirani R, Chu G (2001) Significance analysis of microarrays applied to the ionizing radiation response. *Proc Natl Acad Sci U S A* 98:5116-5121.

Whitfield ML, Sherlock G, Saldanha AJ, Murray JI, Ball CA, Alexander KE, *et al.* (2002) Identification of genes periodically expressed in the human cell cycle and their expression in tumors. *Mol Biol Cell* 13:1977-2000.

**Supplementary Data File S1: Top Differentially Regulated SAM analysis, 6 Months vs Base**

Forearm SAM analysis (FDR < 4.6%)	
859193 ^ C3 ^ Complement component 3 ^ Hs.529053 ^ NM_000064 ^ 718	
697000 ^ OLFM1 ^ Olfactomedin 1 ^ Hs.522484 ^ NM_006334 ^ 10439	
857676 ^ ETS2 ^ V-ets erythroblastosis virus E26 oncogene homolog 2 (avian) ^ Hs.517296 ^ NM_005239 ^ 2114	
866997 ^ GTF2E2 ^ General transcription factor IIE, polypeptide 2, beta 34kDa ^ Hs.77100 ^ NM_002095 ^ 2961	
683877 ^ CDC25B ^ Cell division cycle 25B ^ Hs.153752 ^ NM_021873 ^ 994	
773419 ^ ARK5 ^ AMP-activated protein kinase family member 5 ^ Hs.524692 ^ NM_014840 ^ 9891	
685859 ^ NFKBIE ^ Nuclear factor of kappa light polypeptide gene enhancer in B-cells inhibitor, epsilon ^ Hs.458276 ^ NM_00455	
682131 ^ GPX1 ^ Glutathione peroxidase 1 ^ Hs.76686 ^ NM_201397 ^ 2876	
854760 ^ COCH ^ Coagulation factor C homolog, cochlin (Limulus polyphemus) ^ Hs.21016 ^ NM_004086 ^ 1690	
688410 ^ PAX4 ^ Paired box gene 4 ^ Hs.129706 ^ NM_006193 ^ 5078	
869233 ^ ELK3 ^ ELK3, ETS-domain protein (SRF accessory protein 2) ^ Hs.46523 ^ AW948903 ^ 2004	
854313 ^ SR140 ^ U2-associated SR140 protein ^ Hs.529577 ^ BC040051 ^ 23350	
859844 ^ ^ MRNA; cDNA DKFZp686M03111 (from clone DKFZp686M03111) ^ Hs.209973 ^ BX537816 ^	
867875 ^ GNAZ ^ Guanine nucleotide binding protein (G protein), alpha z polypeptide ^ Hs.526920 ^ NM_002073 ^ 2781	
692278 ^ NSBP1 ^ Nucleosomal binding protein 1 ^ Hs.282204 ^ NM_030763 ^ 79366	
851459 ^ ACDC ^ Adipocyte, C1Q and collagen domain containing ^ Hs.80485 ^ NM_004797 ^ 9370	
697855 ^ FOLR1 ^ Folate receptor 1 (adult) ^ Hs.73769 ^ NM_016725 ^ 2348	

Forearm and Back SAM analysis (FDR < 5.87%)	
842656 ^ ^ ^ ^ NM_001040077 ^	
866997 ^ GTF2E2 ^ General transcription factor IIE, polypeptide 2, beta 34kDa ^ Hs.77100 ^ NM_002095 ^ 2961	
859193 ^ C3 ^ Complement component 3 ^ Hs.529053 ^ NM_000064 ^ 718	
693675 ^ DOCK11 ^ Deducator of cytokinesis 11 ^ Hs.368203 ^ NM_144658 ^ 139818	
691543 ^ ^ ^ ^ NM_001040077 ^	
866825 ^ ADAMTS4 ^ A disintegrin-like and metalloprotease (reprolysin type) with thrombospondin type 1 motif, 4 ^ Hs.211604 ^	
843793 ^ ^ ^ ^ NR_002196 ^	
691834 ^ LOXL2 ^ Lysyl oxidase-like 2 ^ Hs.116479 ^ NM_002318 ^ 4017	
843489 ^ THBS4 ^ Thrombospondin 4 ^ Hs.211426 ^ NM_003248 ^ 7060	
682131 ^ GPX1 ^ Glutathione peroxidase 1 ^ Hs.76686 ^ NM_201397 ^ 2876	
690937 ^ ICAM2 ^ Intercellular adhesion molecule 2 ^ Hs.431460 ^ NM_000873 ^ 3384	
691907 ^ PCOLCE2 ^ Procollagen C-endopeptidase enhancer 2 ^ Hs.8944 ^ NM_013363 ^ 26577	
687738 ^ COL4A2 ^ Collagen, type IV, alpha 2 ^ Hs.508716 ^ NM_001846 ^ 1284	
684371 ^ CDO1 ^ Cysteine dioxygenase, type I ^ Hs.442378 ^ NM_001801 ^ 1036	
865995 ^ EHD2 ^ EH-domain containing 2 ^ Hs.325650 ^ NM_014601 ^ 30846	
688198 ^ RASD1 ^ RAS, dexamethasone-induced 1 ^ Hs.25829 ^ NM_016084 ^ 51655	

**Supplementary Data File S2: Genes correlated with change in CD20+ positive B cell**

<b>Gene Symbol, Description, Acession, LocusLink ID</b>
LCP1 Lymphocyte cytosolic protein 1 (L-plastin) NM_002298 3936
PRKCB1 Protein kinase C, beta 1 NM_002738 5579
ARK5 AMP-activated protein kinase family member 5 NM_014840 9891
FLJ10357 Hypothetical protein FLJ10357 NM_018071 55701
TNFRSF8 Tumor necrosis factor receptor superfamily, member 8 NM_001243 943
RBM14 RNA binding motif protein 14 NM_006328 10432
AASDH 2-aminoadipic 6-semialdehyde dehydrogenase BG209258 132949
C2F C2f protein NM_006331 10436
A_24_P698376
NDFIP1 Nedd4 family interacting protein 1 NM_030571 80762
ALOX5 Arachidonate 5-lipoxygenase NM_000698 240
KIAA1272 KIAA1272 protein AK026194 57186
C3 Complement component 3 NM_000064 718
Homo sapiens, clone IMAGE:5299888, mRNA BC039397
ENST00000277858
TUBB Tubulin, beta polypeptide NM_178014 203068
LOC126208 Hypothetical protein LOC126208 NM_001002836 126208
SLA Src-like-adaptor NM_006748 6503
PSARL Presenilin associated, rhomboid-like NM_018622 55486
MGC11324 Hypothetical protein MGC11324 NM_032717 84803
NM_016265
XTP3TPA XTP3-transactivated protein A NM_024096 79077
RPS6KA3 Ribosomal protein S6 kinase, 90kDa, polypeptide 3 NM_004586 6197
CTSS Cathepsin S NM_004079 1520
ICAM2 Intercellular adhesion molecule 2 NM_000873 3384
SLC43A1 Solute carrier family 43, member 1 NM_003627 8501
CD83 CD83 antigen (activated B lymphocytes, immunoglobulin superfamily) NM_004233
SF3A1 Splicing factor 3a, subunit 1, 120kDa NM_005877 10291
TOR1A Torsin family 1, member A (torsin A) NM_000113 1861
FLJ10774 N-acetyltransferase-like protein NM_024662 55226
USP34 Ubiquitin specific protease 34 NM_014709 9736
CD33 CD33 antigen (gp67) NM_001772 945
MAP1B Microtubule-associated protein 1B CR595522 4131
KLHL12 Kelch-like 12 (Drosophila) NM_021633 59349
BTG1 B-cell translocation gene 1, anti-proliferative NM_001731 694
FBL Fibrillarin NM_001436 2091
LASS2 LAG1 longevity assurance homolog 2 (S. cerevisiae) NM_181746 29956
CD53 CD53 antigen NM_000560 963
ARHGDI1 Rho GDP dissociation inhibitor (GDI) beta NM_001175 397
DKFZP547E1010 DKFZP547E1010 protein AF318362 26097
TRA16 TR4 orphan receptor associated protein TRA16 NM_176880 126382
MAP3K14 Mitogen-activated protein kinase kinase 14 NM_003954 9020
XM_933879
STOM Stomatin NM_198194 2040
MK2S4 Protein kinase substrate MK2S4 NM_052862 92241
CCND2 Cyclin D2 NM_001759 894
PSCDBP Pleckstrin homology, Sec7 and coiled-coil domains, binding protein NM_004288
A_24_P75700
WFS1 Wolfram syndrome 1 (wolframin) NM_006005 7466
MGC14327 Hypothetical protein MGC14327 NM_053045 94107

LRMP Lymphoid-restricted membrane protein NM_006152 4033
ANXA11 Annexin A11 NM_145869 311
CWF19L1 CWF19-like 1, cell cycle control (S. pombe) NM_018294 55280
A_24_P627678
ANGPT1 Angiotensinogen 1 NM_001146 284
LDHB Lactate dehydrogenase B NM_002300 3945
EPAS1 Endothelial PAS domain protein 1 NM_001430 2034
COPG Coatamer protein complex, subunit gamma NM_016128 22820
C12orf2 Chromosome 12 open reading frame 2 AY665468 11228
SNX3 Sorting nexin 3 NM_003795 8724
XRCC5 X-ray repair complementing defective repair in Chinese hamster cells 5 (double-strand break repair protein) NM_005050 4131
NUP93 Nucleoporin 93kDa NM_014669 9688
ACSL4 Acyl-CoA synthetase long-chain family member 4 NM_004458 2182
LIF Leukemia inhibitory factor (cholinergic differentiation factor) NM_002309 3976
KIAA0870 KIAA0870 protein NM_014957 22898
UBADC1 Ubiquitin associated domain containing 1 NM_016172 10422
FLJ10315 Hypothetical protein FLJ10315 NM_018056 55116
MAP1B Microtubule-associated protein 1B NM_005909 4131
DERL1 Der1-like domain family, member 1 NM_024295 79139
A_24_P161655
CD97 CD97 antigen NM_078481 976
PTPN13 Protein tyrosine phosphatase, non-receptor type 13 (APO-1/CD95 (Fas)-associated protein 2) NM_005050 4131
FER1L3 Fer-1-like 3, myoferlin (C. elegans) NM_013451 26509
STK17B Serine/threonine kinase 17b (apoptosis-inducing) NM_004226 9262
THADA Thyroid adenoma associated NM_022065 63892
C14orf123 Chromosome 14 open reading frame 123 NM_014169 29082
A_23_P255111
ZNF219 Zinc finger protein 219 NM_016423 51222
MGC20481 Hypothetical protein MGC20481 NM_052849 90416
THC2314239
CASP10 Caspase 10, apoptosis-related cysteine protease NM_032977 843
TOR3A Torsin family 3, member A NM_022371 64222
YLP1 YLP motif containing 1 BC023570 56252
ITGB2 Integrin, beta 2 (antigen CD18 (p95), lymphocyte function-associated antigen 1; membrane protein 1) NM_001006634 55114
MYST2 MYST histone acetyltransferase 2 NM_007067 11143
THC2365158
VPS18 Vacuolar protein sorting protein 18 NM_020857 57617
CP Ceruloplasmin (ferroxidase) NM_000096 1356
SF3B3 Splicing factor 3b, subunit 3, 130kDa NM_012426 23450
POLDIP3 Polymerase (DNA-directed), delta interacting protein 3 NM_032311 84271
PRKWNK1 Protein kinase, lysine deficient 1 AB002342 65125
JAM2 Junctional adhesion molecule 2 NM_021219 58494
MYO10 Myosin X NM_012334 4651
ARHGAP17 Rho GTPase activating protein 17 NM_001006634 55114
TPT1 Tumor protein, translationally-controlled 1 NM_003295 7178
MGLL Monoglyceride lipase NM_007283 11343
IGJ Immunoglobulin J polypeptide, linker protein for immunoglobulin alpha and mu polypeptide chain NM_001006634 55114
A_23_P125109
MTCH1 Mitochondrial carrier homolog 1 (C. elegans) NM_014341 23787
SLC39A1 Solute carrier family 39 (zinc transporter), member 1 NM_014437 27173
NIP30 NEFA-interacting nuclear protein NIP30 NM_024946 80011
TM7SF3 Transmembrane 7 superfamily member 3 NM_016551 51768

HLA-F Major histocompatibility complex, class I, F NM_018950 3134
ENST00000383620
PDE2A Phosphodiesterase 2A, cGMP-stimulated NM_002599 5138
LTB Lymphotoxin beta (TNF superfamily, member 3) NM_002341 4050
CCND1 Cyclin D1 (PRAD1: parathyroid adenomatosis 1) NM_053056 595
RPL7A Ribosomal protein L7a NM_000972 6130
ZFP36 Zinc finger protein 36, C3H type, homolog (mouse) NM_003407 7538
A_24_P118422
PRCP Prolylcarboxypeptidase (angiotensinase C) NM_199418 5547
POLR3B Polymerase (RNA) III (DNA directed) polypeptide B NM_018082 55703
TPM3 Tropomyosin 3 NM_153649 7170
PSCD4 Pleckstrin homology, Sec7 and coiled-coil domains 4 NM_013385 27128
KIAA1787 G protein pathway suppressor 2 NM_004489 84461
A_24_P264597
UXT Ubiquitously-expressed transcript NM_004182 8409
PRDX1 Peroxiredoxin 1 NM_002574 5052
LOC126295 Hypothetical protein LOC126295 NM_173480 126295

**s found in Immunohistochem****CD20 Skin Correlation**

0.742629542
0.668818617
0.660770446
0.656611358
0.646395674
0.640118651
0.630398781
0.621347496
0.603892546
0.603876771
0.602961839
0.602262961
0.601813065
0.599098543
0.595629176
0.593405906
0.590504429
0.589385722
0.586555164
0.583759312
0.581672004
0.581234648
0.576526426
0.576249283
0.575816175
0.575110406
0.575051981
0.574437925
0.574237847
0.573200305
0.565794017
0.56565121
0.561849228
0.560314263
0.559631735
0.559454772
0.558244029
0.554642413
0.552780418
0.552725423
0.552293051
0.551894419
0.551756888
0.549695154
0.549284927
0.548993292
0.548443302
0.547769108
0.547363592
0.545243182

0.542111791
0.542029594
0.541652017
0.540394247
0.539899046
0.539791471
0.539372628
0.537285623
0.536944695
0.536651194
0.536109456
0.535120163
0.534778556
0.534293743
0.533883632
0.533740244
0.529871234
0.529688842
0.529473878
0.529167054
0.528614972
0.527497416
0.527443734
0.527165153
0.526862439
0.526714141
0.525648114
0.525604697
0.525069896
0.524083116
0.52161047
0.520734532
0.52012431
0.51934293
0.518394165
0.517436469
0.515479635
0.515427824
0.514281934
0.513747155
0.513622899
0.512675877
0.511865529
0.510032339
0.509414047
0.509334303
0.508967776
0.50883488
0.507822795
0.507382977
0.507303306
0.507093191



0.506992465
0.50622238
0.505158885
0.504981369
0.504798738
0.504648555
0.50436297
0.504007049
0.503953898
0.50391122
0.503375808
0.50259553
0.502543376
0.500563502
0.500440344
0.500435368
0.500361059

**ical Analysis of Skin biopsies**

**Supplementary Figure S3: Gene Ontology Biological processes associated with genes in dSSc subsets**

Category	Term	Count	%	PValue
GOTERM_BP_ALL	GO:0044255~cellular lipid metabolic process	38	14.07%	9.70E-14
GOTERM_BP_ALL	GO:0006629~lipid metabolic process	41	15.19%	4.81E-13
GOTERM_BP_ALL	GO:0032787~monocarboxylic acid metabolic process	23	8.52%	4.92E-12
GOTERM_BP_ALL	GO:0019752~carboxylic acid metabolic process	33	12.22%	2.54E-11
GOTERM_BP_ALL	GO:0006082~organic acid metabolic process	33	12.22%	2.91E-11
GOTERM_BP_ALL	GO:0006631~fatty acid metabolic process	19	7.04%	5.27E-11
Category	Term	Count	%	PValue
GOTERM_BP_ALL	GO:0016125~sterol metabolic process	11	4.07%	3.99E-07
GOTERM_BP_ALL	GO:0008203~cholesterol metabolic process	10	3.70%	1.19E-06
GOTERM_BP_ALL	GO:0016126~sterol biosynthetic process	7	2.59%	7.17E-06
GOTERM_BP_ALL	GO:0006695~cholesterol biosynthetic process	6	2.22%	2.78E-05
GOTERM_BP_ALL	GO:0008202~steroid metabolic process	12	4.44%	7.18E-05
GOTERM_BP_ALL	GO:0006694~steroid biosynthetic process	8	2.96%	1.84E-04
Category	Term	Count	%	PValue
GOTERM_BP_ALL	GO:0006066~alcohol metabolic process	21	7.78%	3.18E-08

Genes	List Total	Pop Hits	Pop Total	Fold Enric	Benjamini
FADS1, H	218	624	15360	4.290755	5.09E-10
ACAT2, F	218	764	15360	3.781161	1.26E-09
GPT, FAD	218	244	15360	6.6416	8.62E-09
FADS1, S	218	572	15360	4.064926	3.33E-08
FADS1, S	218	575	15360	4.043718	3.06E-08
FADS1, S	218	175	15360	7.649803	4.61E-08
Genes	List Total	Pop Hits	Pop Total	Fold Enric	Benjamini
INSIG1, H	218	87	15360	8.908573	2.33E-04
INSIG1, H	218	76	15360	9.270884	6.26E-04
HMGCS1,	218	34	15360	14.50621	0.003419
HMGCS1,	218	26	15360	16.2597	0.012078
INSIG1, H	218	187	15360	4.521415	0.026596
HMGCS1,	218	84	15360	6.710354	0.062345
Genes	List Total	Pop Hits	Pop Total	Fold Enric	Benjamini
GPT, PPA	218	322	15360	4.595134	2.39E-05

Category	Term	Count
GOTERM_BP_ALL	GO:0007067~mitosis	28
GOTERM_BP_ALL	GO:0000087~M phase of mitotic cell cycle	28
GOTERM_BP_ALL	GO:0000279~M phase	29
GOTERM_BP_ALL	GO:0000278~mitotic cell cycle	28
GOTERM_BP_ALL	GO:0022403~cell cycle phase	29
GOTERM_BP_ALL	GO:0051301~cell division	24
GOTERM_BP_ALL	GO:0007049~cell cycle	38
GOTERM_BP_ALL	GO:0022402~cell cycle process	34
GOTERM_BP_ALL	GO:0000074~regulation of progression through cell cycle	16
GOTERM_BP_ALL	GO:0051726~regulation of cell cycle	16
Category	Term	Count
GOTERM_BP_ALL	GO:0007017~microtubule-based process	11
GOTERM_BP_ALL	GO:0006996~organelle organization and biogenesis	24
GOTERM_BP_ALL	GO:0007010~cytoskeleton organization and biogenesis	15
Category	Term	Count
GOTERM_BP_ALL	GO:0000226~microtubule cytoskeleton organization and biogenesis	8
GOTERM_BP_ALL	GO:0007017~microtubule-based process	11
GOTERM_BP_ALL	GO:0007051~spindle organization and biogenesis	5
Category	Term	Count
GOTERM_BP_ALL	GO:0007059~chromosome segregation	8
GOTERM_BP_ALL	GO:0051303~establishment of chromosome localization	4
GOTERM_BP_ALL	GO:0050000~chromosome localization	4
GOTERM_BP_ALL	GO:0000070~mitotic sister chromatid segregation	5
GOTERM_BP_ALL	GO:0000819~sister chromatid segregation	5
GOTERM_BP_ALL	GO:0051276~chromosome organization and biogenesis	12
GOTERM_BP_ALL	GO:0051310~metaphase plate congression	3
Category	Term	Count
GOTERM_BP_ALL	GO:0006974~response to DNA damage stimulus	12
GOTERM_BP_ALL	GO:0009719~response to endogenous stimulus	13
GOTERM_BP_ALL	GO:0006259~DNA metabolic process	19
Category	Term	Count
GOTERM_BP_ALL	GO:0007088~regulation of mitosis	6

%	PValue	Genes
19.18%	1.63E-25	PLK1, CDCA8, CDC2, CEP55, PBK, CENPF, TPX2, ASPM, CENPE, SPC25, CDC20, M
19.18%	2.08E-25	PLK1, CDCA8, CDC2, CEP55, PBK, CENPF, TPX2, ASPM, CENPE, SPC25, CDC20, M
19.86%	4.89E-24	PLK1, CDCA8, RAD54B, CDC2, CEP55, PBK, CENPF, TPX2, ASPM, CENPE, SPC25,
19.18%	1.41E-21	PLK1, CDCA8, CDC2, CEP55, PBK, CENPF, TPX2, ASPM, CENPE, SPC25, CDC20, M
19.86%	1.81E-21	PLK1, CDCA8, RAD54B, CDC2, CEP55, PBK, CENPF, TPX2, ASPM, CENPE, SPC25,
16.44%	2.03E-19	CDCA8, CDC2, WEE1, CEP55, ANLN, CCNA2, NUF2, CENPF, ASPM, CENPJ, KIF11,
26.03%	7.53E-19	PLK1, RAD54B, CDCA8, CDC2, MAP2K6, MYBL2, CEP55, PBK, TPX2, CENPF, ASPM
23.29%	1.48E-17	PLK1, CDCA8, RAD54B, CDC2, MAP2K6, MYBL2, CEP55, PBK, TPX2, CENPF, ASPM
10.96%	6.30E-06	PLK1, CDC45L, MAP2K6, CDC2, MYBL2, WEE1, ANLN, DLG7, CCNA2, CENPF, BRO
10.96%	6.75E-06	PLK1, CDC45L, MAP2K6, CDC2, MYBL2, WEE1, ANLN, DLG7, CCNA2, CENPF, BRO
%	PValue	Genes
7.53%	4.69E-06	KIF2C, KIF11, CENPJ, CENPE, BRCA1, KIF20A, SPAG5, NDC80, UBE2C, CTTNBP2,
16.44%	1.40E-05	NEFH, EP400, BLM, KIF20A, ANK1, ANLN, DLG7, HCG_2029577, PTTG2, KIF2C, CE
10.27%	2.83E-05	NEFH, ANK1, KIF20A, ANLN, HCG_2029577, KIF2C, CENPJ, KIF11, CENPE, BRCA1,
%	PValue	Genes
5.48%	2.39E-06	KIF2C, KIF11, CENPJ, SPAG5, NDC80, UBE2C, CTTNBP2, AURKA,
7.53%	4.69E-06	KIF2C, KIF11, CENPJ, CENPE, BRCA1, KIF20A, SPAG5, NDC80, UBE2C, CTTNBP2,
3.42%	1.19E-05	KIF11, SPAG5, NDC80, UBE2C, AURKA,
%	PValue	Genes
5.48%	3.58E-07	CENPF, CENPE, BRCA1, DLG7, NDC80, NCAPG, CDCA5, NUF2,
2.74%	7.43E-06	CENPF, CENPE, DLG7, CDCA5,
2.74%	7.43E-06	CENPF, CENPE, DLG7, CDCA5,
3.42%	7.24E-05	CENPE, DLG7, NDC80, NCAPG, CDCA5,
3.42%	8.23E-05	CENPE, DLG7, NDC80, NCAPG, CDCA5,
8.22%	1.42E-04	CENPF, NEFH, EP400, CENPE, BLM, CHAF1B, DLG7, NDC80, GSG2, NCAPG, CDC,
2.05%	3.13E-04	CENPF, CENPE, CDCA5,
%	PValue	Genes
8.22%	2.45E-05	RAD54B, UHRF1, BLM, CHAF1B, CDC2, MAP2K6, BRCA1, TYMS, DTL, FANCI, CCN
8.90%	3.75E-05	UHRF1, RAD54B, BLM, MAP2K6, CDC2, CCNA2, CHAF1B, BRCA1, DTL, TYMS, FAN
13.01%	4.76E-05	CDC45L, RAD54B, UHRF1, NEFH, EP400, BLM, ORC6L, PTTG2, TK1, DNMT3B, DNI
%	PValue	Genes
4.11%	1.56E-04	CENPF, CDC2, ANLN, DLG7, UBE2C, CCNA2,

List Total	Pop Hits	Pop Total	Fold Enrichment	Benjamini
113	227	15360	16.7666	8.59E-22
113	229	15360	16.62016	5.46E-22
113	287	15360	13.73501	8.56E-21
113	318	15360	11.96861	1.85E-18
113	356	15360	11.07288	1.91E-18
113	245	15360	13.31551	1.78E-16
113	894	15360	5.777751	5.65E-16
113	749	15360	6.170351	9.73E-15
113	526	15360	4.134729	0.002755
113	529	15360	4.11128	0.002723
List Total	Pop Hits	Pop Total	Fold Enrichment	Benjamini
113	220	15360	6.79646	0.002238
113	1195	15360	2.729959	0.004324
113	526	15360	3.876308	0.007802
List Total	Pop Hits	Pop Total	Fold Enrichment	Benjamini
113	83	15360	13.10161	0.001253
113	220	15360	6.79646	0.002238
113	20	15360	33.9823	0.003887
List Total	Pop Hits	Pop Total	Fold Enrichment	Benjamini
113	63	15360	17.26085	2.09E-04
113	6	15360	90.61947	0.002599
113	6	15360	90.61947	0.002599
113	31	15360	21.92407	0.017144
113	32	15360	21.23894	0.018623
113	394	15360	4.139976	0.030583
113	4	15360	101.9469	0.061333
List Total	Pop Hits	Pop Total	Fold Enrichment	Benjamini
113	324	15360	5.034415	0.007117
113	403	15360	4.384813	0.009798
113	860	15360	3.003087	0.011847
List Total	Pop Hits	Pop Total	Fold Enrichment	Benjamini
113	70	15360	11.65107	0.032335

Functional Group 1				
Category	Term	Count	%	PValue
GOTERM_BP_ALL	GO:0002376~immune system process	72	14.26%	6.65E-11
GOTERM_BP_ALL	GO:0006955~immune response	59	11.68%	2.82E-09
GOTERM_BP_ALL	GO:0050896~response to stimulus	128	25.35%	1.38E-07
Functional Group 2				
Category	Term	Count	%	PValue
GOTERM_BP_ALL	GO:0009611~response to wounding	39	7.72%	1.51E-10
GOTERM_BP_ALL	GO:0006950~response to stress	66	13.07%	8.39E-10
GOTERM_BP_ALL	GO:0009605~response to external stimulus	46	9.11%	5.40E-09
GOTERM_BP_ALL	GO:0006952~defense response	41	8.12%	5.03E-08
GOTERM_BP_ALL	GO:0006954~inflammatory response	28	5.54%	5.25E-08
Functional Group 3				
Category	Term	Count	%	PValue
GOTERM_BP_ALL	GO:0032502~developmental process	143	28.32%	4.87E-10
GOTERM_BP_ALL	GO:0048513~organ development	62	12.28%	9.94E-06
GOTERM_BP_ALL	GO:0007275~multicellular organismal development	97	19.21%	1.50E-05
GOTERM_BP_ALL	GO:0048856~anatomical structure development	90	17.82%	2.16E-05
GOTERM_BP_ALL	GO:0048731~system development	73	14.46%	2.24E-04
GOTERM_BP_ALL	GO:0032501~multicellular organismal process	122	24.16%	0.016569
Category	Term	Count	%	PValue
GOTERM_BP_ALL	GO:0006915~apoptosis	48	9.50%	2.61E-07
GOTERM_BP_ALL	GO:0012501~programmed cell death	48	9.50%	3.39E-07
GOTERM_BP_ALL	GO:0008219~cell death	48	9.50%	1.50E-06
GOTERM_BP_ALL	GO:0016265~death	48	9.50%	1.50E-06
GOTERM_BP_ALL	GO:0048468~cell development	62	12.28%	3.96E-06
GOTERM_BP_ALL	GO:0042981~regulation of apoptosis	35	6.93%	4.20E-06
GOTERM_BP_ALL	GO:0043067~regulation of programmed cell death	35	6.93%	5.31E-06
GOTERM_BP_ALL	GO:0048869~cellular developmental process	78	15.45%	5.45E-05
GOTERM_BP_ALL	GO:0030154~cell differentiation	78	15.45%	5.45E-05
Category	Term	Count	%	PValue
GOTERM_BP_ALL	GO:0006928~cell motility	30	5.94%	4.23E-06
GOTERM_BP_ALL	GO:0051674~localization of cell	30	5.94%	4.23E-06
GOTERM_BP_ALL	GO:0016477~cell migration	18	3.56%	0.001185
Category	Term	Count	%	PValue
GOTERM_BP_ALL	GO:0006817~phosphate transport	16	3.17%	3.17E-08
GOTERM_BP_ALL	GO:0015698~inorganic anion transport	17	3.37%	8.48E-06
GOTERM_BP_ALL	GO:0006820~anion transport	17	3.37%	1.00E-04
Category	Term	Count	%	PValue
GOTERM_BP_ALL	GO:0007243~protein kinase cascade	29	5.74%	3.27E-06
GOTERM_BP_ALL	GO:0009966~regulation of signal transduction	34	6.73%	3.89E-05
GOTERM_BP_ALL	GO:0009967~positive regulation of signal transduction	15	2.97%	7.18E-05
GOTERM_BP_ALL	GO:0007249~I-kappaB kinase/NF-kappaB cascade	14	2.77%	8.93E-05
GOTERM_BP_ALL	GO:0043123~positive regulation of I-kappaB kinase activity	11	2.18%	2.47E-04
GOTERM_BP_ALL	GO:0043122~regulation of I-kappaB kinase activity	11	2.18%	4.77E-04
Category	Term	Count	%	PValue
GOTERM_BP_ALL	GO:0001944~vasculature development	19	3.76%	4.55E-06



GOTERM_BP_ALL	GO:0048514~blood vessel morphogenesis	17	3.37%	1.16E-05
GOTERM_BP_ALL	GO:0001568~blood vessel development	18	3.56%	1.44E-05
GOTERM_BP_ALL	GO:0001525~angiogenesis	15	2.97%	3.41E-05
GOTERM_BP_ALL	GO:0048646~anatomical structure formation	16	3.17%	1.09E-04
GOTERM_BP_ALL	GO:0009887~organ morphogenesis	24	4.75%	9.77E-04
Category	Term	Count	%	PValue
GOTERM_BP_ALL	GO:0042981~regulation of apoptosis	35	6.93%	4.20E-06
GOTERM_BP_ALL	GO:0043067~regulation of programmed cell	35	6.93%	5.31E-06
Category	Term	Count	%	PValue
GOTERM_BP_ALL	GO:0009607~response to biotic stimulus	22	4.36%	1.32E-04
GOTERM_BP_ALL	GO:0009615~response to virus	11	2.18%	3.47E-04
Category	Term	Count	%	PValue
GOTERM_BP_ALL	GO:0065007~biological regulation	176	34.85%	3.69E-04
Category	Term	Count	%	PValue
GOTERM_BP_ALL	GO:0006959~humoral immune response	11	2.18%	2.58E-05
GOTERM_BP_ALL	GO:0002541~activation of plasma proteins d	7	1.39%	3.17E-04
GOTERM_BP_ALL	GO:0006956~complement activation	7	1.39%	3.17E-04
GOTERM_BP_ALL	GO:0002526~acute inflammatory response	9	1.78%	9.35E-04
GOTERM_BP_ALL	GO:0002455~humoral immune response me	6	1.19%	9.88E-04
GOTERM_BP_ALL	GO:0002252~immune effector process	11	2.18%	9.89E-04
Category	Term	Count	%	PValue
GOTERM_BP_ALL	GO:0030198~extracellular matrix organizatio	8	1.58%	7.50E-04
Category	Term	Count	%	PValue
GOTERM_BP_ALL	GO:0042771~DNA damage response, signal	4	0.79%	6.36E-04
Category	Term	Count	%	PValue
GOTERM_BP_ALL	GO:0007242~intracellular signaling cascade	61	12.08%	0.001232

Genes	List Total	Pop Hits	Pop Total	Fold Enrich	Benjamini
PXDN, IFIT1, IFITM2, HLA-A, PURB, MR1, MLF1, BPV	417	1165	15360	2.276469	3.49E-07
PXDN, IFIT1, IFITM2, HLA-A, MR1, IFITM1, HLA-G, IL	417	938	15360	2.316884	2.96E-06
SERP1, IFIT1, CMTM3, IFITM2, HLA-A, HSPA5, MR1	417	3066	15360	1.537776	7.25E-05
Genes	List Total	Pop Hits	Pop Total	Fold Enrich	Benjamini
PRKCA, APOL2, NMI, PROCR, IRF7, PLSCR1, FGF7	417	431	15360	3.333055	3.96E-07
SERP1, PXDN, SMC6, MUS81, HSPA5, APOL2, LOC	417	1081	15360	2.248917	1.10E-06
CMTM3, PRKCA, APOL2, NMI, PROCR, IRF7, PLSCR	417	644	15360	2.631038	4.73E-06
PRKCA, APOL2, NMI, PROCR, TAP1, IRF7, HLA-G, IL	417	577	15360	2.617358	3.30E-05
PRKCA, NMI, APOL2, PROCR, IRF7, C3, B4GALT1, F	417	301	15360	3.426468	3.07E-05
Genes	List Total	Pop Hits	Pop Total	Fold Enrich	Benjamini
IGFBP7, FEZ2, SOCS3, PERP, HSPA5, PURB, VCAN	417	3262	15360	1.614757	8.53E-07
CASP7, PURB, MLF1, ODC1, SRGN, BPGM, COL6A3	417	1282	15360	1.781389	0.002007
FEZ2, PURB, MLF1, VCAN, SFRP2, CDH13, NRP1, H	417	2349	15360	1.521051	0.002541
IGFBP7, FEZ2, SOCS3, PURB, CASP7, MLF1, ODC1	417	2153	15360	1.539762	0.003536
FEZ2, PURB, CASP7, MLF1, ODC1, SRGN, BPGM, C	417	1760	15360	1.527796	0.025762
FEZ2, PURB, MLF1, VCAN, SFRP2, CDH13, NRP1, H	417	3759	15360	1.195481	0.530809
Genes	List Total	Pop Hits	Pop Total	Fold Enrich	Benjamini
DYRK2, SOCS3, CARD6, BIRC3, PIM1, PRKCA, SUL	417	784	15360	2.255175	1.14E-04
DYRK2, SOCS3, CARD6, BIRC3, PIM1, PRKCA, SUL	417	791	15360	2.235218	1.37E-04
DYRK2, SOCS3, CARD6, BIRC3, PIM1, PRKCA, SUL	417	834	15360	2.119973	5.26E-04
DYRK2, SOCS3, CARD6, BIRC3, PIM1, PRKCA, SUL	417	834	15360	2.119973	5.26E-04
FEZ2, SOCS3, SULF1, HSPA5, DRAM, PERP, CASP	417	1245	15360	1.83433	0.001094
DYRK2, CARD6, SOCS3, BIRC3, PIM1, PRKCA, HSP	417	538	15360	2.396299	0.001102
DYRK2, CARD6, SOCS3, BIRC3, PIM1, PRKCA, HSP	417	544	15360	2.369869	0.001161
FEZ2, SOCS3, SULF1, PERP, DRAM, HSPA5, PURB	417	1835	15360	1.565719	0.007501
FEZ2, SOCS3, SULF1, PERP, DRAM, HSPA5, PURB	417	1835	15360	1.565719	0.007501
Genes	List Total	Pop Hits	Pop Total	Fold Enrich	Benjamini
FEZ2, PRKCA, CENTD2, ARPC1B, LAMC1, B4GALT	417	421	15360	2.624789	0.001057
FEZ2, PRKCA, CENTD2, ARPC1B, LAMC1, B4GALT	417	421	15360	2.624789	0.001057
VAV2, LAMB1, FEZ2, SPON2, TNFRSF12A, PRKCA,	417	271	15360	2.446574	0.097107
Genes	List Total	Pop Hits	Pop Total	Fold Enrich	Benjamini
C1QTNF5, COL15A1, COL6A1, COL4A2, COL6A3, C	417	94	15360	6.269708	2.38E-05
C1QTNF5, COL15A1, COL6A1, COL4A2, COL6A3, C	417	162	15360	3.865352	0.00178
C1QTNF5, COL15A1, COL6A1, COL4A2, COL6A3, C	417	198	15360	3.162561	0.01274
Genes	List Total	Pop Hits	Pop Total	Fold Enrich	Benjamini
SOCS3, PRKCA, NMI, WNT5A, ECOP, TGFB3, STAT	417	393	15360	2.71807	9.55E-04
SOCS3, RGS20, PRKCA, TBC1D1, CENTD2, HTRA1	417	573	15360	2.185644	0.005663
LGALS9, CASP1, TNFSF10, TWSG1, SYK, ECOP, C	417	153	15360	3.611229	0.009629
LGALS9, CASP1, TNFSF10, ECOP, STAT1, SECTM1	417	137	15360	3.764113	0.011659
LGALS9, SECTM1, BST2, TNFRSF1A, CASP1, TNFS	417	95	15360	4.265051	0.027869
LGALS9, SECTM1, BST2, TNFRSF1A, CASP1, TNFS	417	103	15360	3.933785	0.047063
Genes	List Total	Pop Hits	Pop Total	Fold Enrich	Benjamini
HEY1, TNFRSF12A, PML, COL15A1, COL4A2, RUNX	417	191	15360	3.664168	0.00104

